Geophys J. R. astr. Soc. (1975) **43**, 269–291.

Autoregressive Representation of Seismic *P*-wave Signals with an Application to the Problem of Short-Period Discriminants

D. Tjøstheim

(Received 1975 April 28)*

Summary

It is shown that seismic *P*-wave signals can be represented by parametric models of autoregressive type. These are models having the form

$$X(t)-a_1 X(t-1)-\ldots-a_p X(t-p) = Z(t)$$

where $X(t)$ is the digitized short-period data time series defined by the *P*-wave signal, and $Z(t)$ is a white noise series. The autoregressive analysis is undertaken for 40 underground nuclear explosions and 45 earthquakes from Eurasia. For each event a separate analysis of the noise preceding the event as well as of the *P*-wave coda has been included. It is found that in most cases a reasonable statistical fit is obtained using a low order autoregressive model. The autoregressive parameters characterize the power spectrum (equivalently, the autocorrelation function) of the *P*-wave signal and form a convenient basis for studying the possibilities of short-period discrimination between nuclear explosions and earthquakes. A preliminary discussion of these possibilities is included.

1. Introduction

With the increased use of digital processing of seismic data an increasing number of problems in statistical seismology involve an analysis of discrete random time series. In a number of cases the time series under study may be considered wide sense stationary (wss) at least within certain time intervals. The second order (second moment) statistical structure of such a time series can be examined using two different methods. The first possibility is an analysis of the series in terms of its autocorrelation function or equivalently its power spectral density. The second possibility consists in trying to fit a parametric model to the given time series.

Lately the parametric method has become increasingly popular. Probably this is due to the recent development of a more effective and systematic approach to parametric model building. We refer to Box & Jenkins (1970) which contain general methods for identification, fitting, estimating and diagnostic checking of general ARMA (autoregressive-moving average) time series models. ARMA models comprise those wss time series $X(t)$ which can be represented as

$$X(t)-a_1 X(t-1)-\ldots-a_p X(t-p) = Z(t)-b_1 Z(t-1)-\ldots-b_q Z(t-q) \qquad (1)$$

* Received in original form 1975 February 13

where $X(t)$ is the observed time series, and $Z(t)$ is a white noise time series such that $E\{X(t)Z(s)\} = 0$ for $s > t$. Similar models exist (Box & Jenkins 1970) for certain classes of non-stationary time series.

Up to now parametric models have mainly been applied in the general fields of engineering and economics. With the exception of Tjøstheim (1975) it appears that no systematic use has been made of such models in statistical seismology. It was demonstrated in Tjøstheim (1975) that the digitized short-period noise at NORSAR can be described with a satisfactory statistical fit by an autoregressive model ($b_1, b_2, \ldots, b_q = 0$ in equation (1)). It is natural to consider next the possibility of fitting an autoregressive model to the discrete time series defined by a digitized P-wave signal. This will be the main topic of this paper.

A parametric representation would be particularly advantageous in cases where it is important to characterize the second-order (equivalently, the power spectral density) properties of the data in terms of a few parameters. The problem of constructing effective short-period discriminants between underground nuclear explosions and shallow earthquakes is such a case. Such discriminants are based on the information contained in the short-period data of a seismic event. If the short-period data time series can be characterized by a few parameters, these should form an ideal basis for the construction of such discriminants. A preliminary study of these possibilities is given in Sections 5 and 6 of this paper.

2. Autoregressive models

To make this paper self-contained, we include in this section a brief review of the properties of autoregressive models. For more details we refer to Box & Jenkins (1970) and Tjøstheim (1975). Let $X(t)$ be a real-valued wss random process in discrete time. The process is said to be autoregressive of order p if $X(t)$ is generated by a difference equation having the form

$$X(t) - a_1 X(t-1) - \ldots - a_p X(t-p) = Z(t). \tag{2}$$

Here $Z(t)$ is a wss white noise process, that is, $E\{Z(t)Z(s)\} = \sigma_z^2 \delta_{ts}$ ($\delta_{ts} = 0$ for $t \neq s$, $\delta_{ts} = 1$ otherwise). Furthermore, it is assumed that $E\{X(t)Z(s)\} = 0$ for $s > t$. If the process $X(t)$ has zero mean, the model (2) contains $p+1$ parameters, the autoregressive coefficients $a_1, a_2, \ldots, a_p$ and the variance $\sigma_z^2 = E\{Z(s)\}^2$ of the residual process $Z(s)$. Once the order p has been determined, standard methods exist for estimating these parameters. For an autoregressive process of order p, the theoretical power spectrum is given (Box & Jenkins 1970) by

$$G(f) = \frac{\sigma_z^2 / f_c}{|1 - a_1 \exp(-\pi i (f/f_c)) - \ldots - a_p \exp(-p\pi i (f/f_c))|^2} \tag{3}$$

for $0 \leqslant f \leqslant f_c$, where i is the imaginary unit, and $f_c = \frac{1}{2}h$ is the cut-off frequency, h being the time interval between samples. It is clear from equation (3) that the shape of the power spectrum is completely determined by the autoregressive coefficients $a_1, a_2, \ldots, a_p$. The parameter σ_z^2 is merely entering as a scaling factor.

3. Data

The list of presumed explosions and earthquakes used in this study is given in Tables 1 and 2. See also Fig. 1. We have chosen to include only events reported by both NORSAR and NOAA (National Oceanic and Atmospheric Administration). All of the events are Eurasian. A large data base with a large variation in epicentre location of presumed explosions is available at NORSAR for this geographical area. Also, the P-wave signals from this area (as recorded by NORSAR) have a large

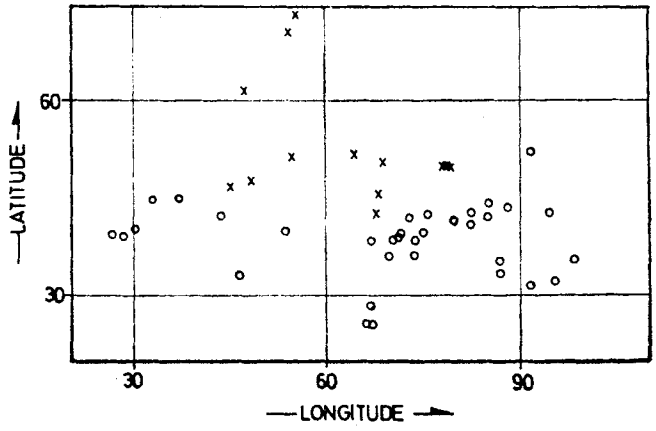

FIG. 1. Geographical distribution of the explosions (crosses) and earthquakes (open circles) of Table 1.

proportion of their energy in the higher frequency bands. This fact results in complex and varied power spectral shapes, thus making them especially interesting for parametric model studies.

The short-period seismic data as processed by NORSAR for the events listed in Tables 1 and 2 are contained on high rate digital tapes, so-called event tapes. To explain the data organization used on these tapes, we have to define first some simple concepts used in the description of a seismic array. The NORSAR seismic array comprises altogether 132 short-period seismometers which are organized in 22 so-called subarrays each containing six seismometers. The seismic data are measured in quantum units, where one quantum unit represents a ground motion of 0·0427 nanometres at 1 Hz. A subarray beam is a phased sum of the six short-period sensors, while an array beam is a phased sum of subarray beams. Using appropriate time delays the subarray (array) beam can be pointed towards the presumed epicentre of a seismic event. For each seismic event the event tape contains the non-filtered subarray beam traces as well as the array beam trace associated with the estimated epicentre of this particular event. The sampling rate is 10 Hz, and each beam trace has a length of 2 mins, that is, each beam trace contains 1200 samples. It should be noted, however, that (approximately) the first 300 samples consist of noise preceding the event. For a more detailed description of the NORSAR array system we refer to Bungum, Husebye & Ringdal (1971).

For the purposes of our analysis we have found it convenient to split each beam trace into five sections; a noise portion, a signal portion and a coda portion which in its turn has been subdivided into three parts. The length of each time window is given in Table 3.

4. Fitting an autoregressive model

The data analysing procedure has been as follows. Each seismic event as recorded digitally is assumed to describe a discrete random time series. Furthermore, within each time window the series is assumed to be wss, and we attempt to fit a model of form (2). In this paper, therefore, the process $X(t)$ of equation (2) will represent the non-filtered seismic data as measured for a certain beam trace and within a particular time window.

To illustrate the analysis we will go through the estimating/fitting procedure in some detail for one 'typical' presumed explosion; no. 22 in the list of presumed

Table 1

NOAA source and identification data for Eurasian presumed explosions. The coefficients $\hat{a}_{31}$, $\hat{a}_{32}$ and $\hat{a}_{33}$ are the estimated 3rd order autoregressive coefficients for the time series defined by the first part of the coda (C1 series) of the subarray beam trace of the events

No.	Date	Origin time (GMT)	Epicentre LA (N)	Epicentre LO (E)	Dist	Depth (km)	m_b	$\hat{a}_{31}$	$\hat{a}_{32}$	$\hat{a}_{33}$
1	1971 June 6	40257	50·0	77·8	37·8	0	5·5	0·82	−0·72	0·18
2	1971 June 19	40358	50·0	77·7	37·7	0	5·5	0·81	−0·55	0·10
3	1971 June 30	35658	50·0	79·1	38·4	0	5·4	0·48	−0·68	0·19
4	1971 July 10	165959	64·2	55·2	20·4	0	5·3	0·82	−0·64	0·12
5	1971 September 19	110007	57·8	41·1	15·6	33	4·5	−0·09	−0·32	−0·26
6	1971 September 27	55955	73·4	55·1	20·6	0	6·4	0·73	−0·27	−0·17
7	1971 October 4	100002	61·6	47·1	17·3	13	5·1	0·07	−0·40	0·08
8	1971 October 9	60257	50·0	77·7	37·7	0	5·4	0·86	−0·75	0·57
9	1971 October 21	60257	50·0	77·6	37·7	0	5·6	0·77	−0·74	0·45
10	1971 October 22	50000	51·6	54·5	25·5	6	5·3	0·60	−0·22	−0·21
11	1971 November 29	60257	49·8	78·1	38·1	0	5·5	1·03	−0·70	0·28
12	1971 December 15	75259	50·0	77·9	37·8	0	4·9	1·32	−0·56	0·14
13	1971 December 22	65956	47·9	48·2	24·9	0	6·0	0·93	−0·66	0·01
14	1971 December 30	62057	49·7	78·1	38·1	0	5·8	0·64	−0·75	0·17
15	1972 February 10	50257	50·0	78·9	38·3	0	5·5	0·85	−0·79	0·36
16	1972 March 10	45657	49·8	78·2	38·1	0	5·5	0·49	−0·58	0·10
17	1972 March 28	42157	49·7	78·2	38·1	0	5·2	0·96	−1·39	0·37
18	1972 June 7	12757	49·8	78·2	38·1	0	5·5	0·28	−0·53	−0·05

Table 1 (*continued*)

19	1972 July 6	10257	49·7	78·0	38·0	0	4·4	1·02	−0·70	0·43
20	1972 August 16	31657	49·8	78·1	38·1	0	5·2	0·70	−0·43	0·05
21	1972 August 26	34657	50·0	77·8	37·8	0	5·5	0·45	−0·70	0·20
22	1972 September 2	85658	50·0	77·7	37·8	0	5·1	0·79	−0·19	0·17
23	1972 October 3	85958	46·8	45·0	24·1	0	5·8	1·57	−1·07	0·18
24	1972 November 2	12658	49·9	78·8	38·3	0	6·2	0·89	−0·78	0·14
25	1972 November 24	90008	52·8	51·1	23·1	33	4·7	0·47	−0·38	0·01
26	1972 November 24	95958	51·8	64·2	30·0	0	5·2	0·46	−0·23	0·01
27	1973 February 16	50258	49·8	78·2	38·1	0	5·6	0·70	−0·63	0·43
28	1973 July 10	12658	49·8	78·1	38·0	0	5·4	0·71	−0·44	−0·08
29	1973 July 23	12258	50·0	78·9	38·3	0	6·3	1·22	−0·74	−0·04
30	1973 August 15	15958	42·7	67·4	37·9	0	5·3	1·25	−0·67	−0·01
31	1973 August 28	25958	50·5	68·4	32·9	0	5·3	0·78	−0·60	0·20
32	1973 September 12	65954	73·3	55·2	20·6	0	6·8	0·22	−0·02	0·15
33	1973 September 19	25957	45·6	67·8	36·0	0	5·2	0·96	−0·81	0·25
34	1973 September 27	65958	70·8	53·9	19·7	0	6·0	0·79	−0·43	−0·07
35	1973 October 26	42658	49·8	78·2	38·1	0	5·3	0·93	−0·39	0·30
36	1973 October 26	55958	53·7	55·4	24·7	0	4·8	0·28	−0·15	0·17
37	1973 December 14	74657	50·0	79·0	38·3	0	6·0	0·69	−0·75	0·26
38	1974 January 30	45702	49·8	78·1	38·0	0	5·4	0·80	−0·37	0·25
39	1974 May 16	30257	49·7	78·2	38·1	0	5·3	0·47	−0·77	0·16
40	1974 May 31	32657	50·0	78·8	38·3	0	5·9	1·16	−0·95	0·24

Table 2

Same as in Table 1 for Eurasian presumed earthquakes

No.	Date	Origin time (GMT)	Epicentre LA (N)	Epicentre LO (E)	Dist	Depth (km)	m_b	$\hat{a}_{31}$	$\hat{a}_{32}$	$\hat{a}_{33}$
1	1971 March 23	95212	41·5	79·3	44·6	33	5·7	1·70	−1·27	0·30
2	1971 March 23	204717	41·5	79·3	44·7	33	6·0	1·73	−1·38	0·42
3	1971 March 24	135418	35·5	98·2	58·4	13	5·8	1·68	−1·37	0·37
4	1971 April 4	13523	38·4	73·3	44·1	33	4·8	1·87	−1·40	0·39
5	1971 June 4	141046	32·2	95·2	59·7	33	5·0	1·37	−1·05	0·24
6	1971 June 15	220413	41·5	79·3	44·6	33	5·6	1·42	−0·77	0·01
7	1971 June 15	231734	41·6	79·2	44·5	33	4·9	1·78	−1·39	0·37
8	1971 June 16	5837	41·5	79·4	44·7	33	5·4	1·79	−1·48	0·45
9	1971 June 16	134651	41·3	79·3	44·8	33	5·1	1·11	−0·54	−0·06
10	1971 June 17	152012	41·3	79·4	44·8	33	4·9	1·62	−1·26	0·37
11	1971 June 19	172303	41·5	79·3	44·6	33	5·2	1·42	−0·86	0·05
12	1971 June 28	195346	42·4	43·3	26·8	34	4·6	1·60	−1·16	0·25
13	1971 July 3	42622	41·3	79·3	44·7	17	4·9	1·48	−1·06	0·24
14	1971 July 30	201314	41·3	79·3	44·8	33	4·5	1·47	−1·19	0·44
15	1971 August 24	163323	52·2	91·4	42·5	33	5·2	1·34	−0·92	0·30
16	1971 October 1	162748	38·6	69·8	42·2	36	4·9	1·60	−1·03	0·22
17	1971 October 28	133057	41·9	72·4	41·0	22	5·5	1·80	−1·31	0·29
18	1971 November 1	52957	44·0	85·0	45·5	33	5·0	1·14	−0·65	0·08
19	1971 November 18	73133	38·3	66·8	41·0	30	5·3	1·61	−1·08	0·26
20	1971 November 19	10001	41·9	72·4	41·0	33	4·9	1·93	−1·46	0·41
21	1972 April 9	41051	42·2	84·6	46·7	33	5·9	1·77	−1·39	0·37

Table 2 (*continued*)

22	1972 April 26	155945	39·5	26·3	23·4	28	4·8	1·48	−1·02	0·18
23	1972 June 10	112911	28·2	66·5	49·2	17	4·5	1·74	−1·35	0·46
24	1972 June 13	5537	33·1	46·3	36·0	27	5·1	1·39	−1·09	0·27
25	1972 June 16	185752	36·0	69·2	44·0	40	4·5	1·04	−0·07	−0·34
26	1972 June 21	50617	40·2	30·0	23·7	33	4·1	1·44	−0·71	0·01
27	1972 July 5	40949	43·6	87·9	47·2	33	4·3	1·25	−0·77	0·15
28	1972 July 22	51040	44·9	36·9	22·1	33	4·6	1·13	−0·93	0·19
29	1972 July 28	153143	31·4	91·4	58·6	33	4·3	1·45	−0·75	0·03
30	1972 August 6	5312	44·7	32·6	20·7	32	4·5	0·71	−0·71	0·03
31	1972 September 2	103739	39·9	53·7	33·5	33	4·9	1·12	−0·71	0·32
32	1972 September 3	83843	39·2	28·1	24·2	16	4·6	2·02	−1·67	0·53
33	1972 September 3	230352	35·9	73·3	46·0	33	5·6	1·72	−1·25	0·25
34	1972 September 17	173749	35·9	73·3	46·0	33	5·4	1·59	−1·04	0·12
35	1972 September 23	72359	25·4	66·7	51·6	10	4·4	1·90	−1·56	0·55
36	1973 January 30	111013	42·7	94·3	50·8	33	4·3	1·62	−0·97	0·25
37	1973 February 5	233049	42·9	82·1	44·9	33	4·5	1·91	−1·16	0·21
38	1973 May 8	110403	39·4	71·0	42·2	33	4·5	1·02	−0·16	−0·09
39	1973 June 10	160842	39·5	74·8	44·0	33	5·2	1·71	−1·41	0·50
40	1973 June 16	223844	41·0	82·0	46·4	33	4·6	1·65	−1·23	0·37
41	1973 July 14	133930	35·3	86·6	53·1	33	5·9	1·74	−1·25	0·28
42	1973 July 26	42023	39·0	70·6	42·4	33	4·1	1·61	−1·08	0·27
43	1973 August 14	182420	25·4	65·7	51·1	33	5·1	1·90	−1·48	0·41
44	1973 September 1	123235	42·6	75·2	41·8	33	4·7	1·55	−0·93	0·17
45	1973 September 8	72544	33·2	86·7	54·8	33	5·5	1·55	−0·83	0·14

Table 3

Number of samples for the five sections of the beam trace obtained by splitting the trace into a noise section, a signal section and three coda sections. The sampling rate is 10 *Hz*

		Sample
N	Noise	0–250
S	Signal	300–365
C1	Coda 1	365–600
C2	Coda 2	600–900
C3	Coda 3	900–1200

explosions, and one 'typical' presumed earthquake; no. 10 in the list of presumed earthquakes (the word 'presumed' will be omitted in the sequel). The time series for one particular subarray (subarray 10C) will be used. We refer to Fig. 2 for a plot of the subarray beam traces. The time series generated by the noise, signal and various coda parts as defined in Table 3 will be referred to as the N, S, C1, C2 and C3 time series respectively. Thus we are trying to fit 10 time series altogether.

The first problem consists in estimating the order p of the time series involved. Let

$$X(t)-a_{k1}X(t-1)-\ldots-a_{kk}X(t-k)=Z(t)$$

be an autoregressive process of order k, where k is allowed to vary. Denote by $\rho(t)$ the autocorrelation function of $X(t)$. It is not difficult to show that the coefficients $a_{k1}, a_{k2}, \ldots, a_{kk}$ satisfy the Yule–Walker equations

$$\begin{bmatrix} 1 & \rho(1) & \rho(2) & \ldots & \rho(k-1) \\ \rho(1) & 1 & \rho(1) & \ldots & \rho(k-2) \\ \cdot & \cdot & \cdot & \ldots & \cdot \\ \cdot & \cdot & \cdot & \ldots & \cdot \\ \cdot & \cdot & \cdot & \ldots & \cdot \\ \rho(k-1) & \rho(k-2) & \rho(k-3) & \ldots & 1 \end{bmatrix} \begin{bmatrix} a_{k1} \\ a_{k2} \\ \cdot \\ \cdot \\ \cdot \\ a_{kk} \end{bmatrix} = \begin{bmatrix} \rho(1) \\ \rho(2) \\ \cdot \\ \cdot \\ \cdot \\ \rho(k) \end{bmatrix}$$

It should be noted that these equations also enter in the construction of the first order prediction error filter, Peacock & Treitel (1969), and in the construction of Burg's 'maximum entropy' spectrum, Lacoss (1971).

The coefficient $A(t)=a_{tt}$ considered as a function of t is called the partial autocorrelation function. An estimate $\hat{A}(t)=\hat{a}_{tt}$ is obtained from

$$\begin{bmatrix} 1 & \hat{\rho}(1) & \hat{\rho}(2) & \ldots & \hat{\rho}(k-1) \\ \hat{\rho}(1) & 1 & \hat{\rho}(1) & \ldots & \hat{\rho}(k-2) \\ \cdot & \cdot & \cdot & \ldots & \cdot \\ \cdot & \cdot & \cdot & \ldots & \cdot \\ \cdot & \cdot & \cdot & \ldots & \cdot \\ \hat{\rho}(k-1) & \hat{\rho}(k-2) & \hat{\rho}(k-3) & \ldots & 1 \end{bmatrix} \begin{bmatrix} \hat{a}_{k1} \\ \hat{a}_{k2} \\ \cdot \\ \cdot \\ \cdot \\ \hat{a}_{kk} \end{bmatrix} = \begin{bmatrix} \hat{\rho}(1) \\ \hat{\rho}(2) \\ \cdot \\ \cdot \\ \cdot \\ \hat{\rho}(k) \end{bmatrix} \tag{4}$$

where

$$\hat{\rho}(k)=\sum_{t=1}^{N-k}X(t)X(t+k)\Big/\sum_{t=1}^{N}[X(t)]^2 \tag{5}$$

and N is the total number of observations, that is, $N=250$, 65, 235, 300 and 300 for the N, S, C1, C2 and C3 time series respectively. It can be shown (Box & Jenkins 1970) that $\hat{A}(t)$ (and $\hat{a}_{ki}$, $i=1,2,\ldots,k$) is a good approximation to the maximum likelihood estimate of $A(t)$ (a_{ki}, $i=1,2,\ldots,k$) if the sample is large.

For an autoregressive process of order p, $A(t)=0$ for $t>p$. Then the standard

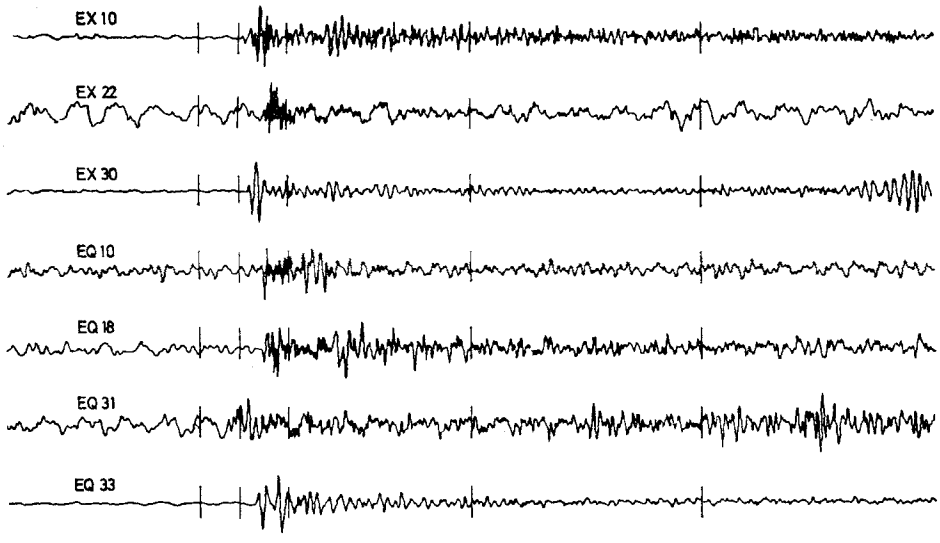

FIG. 2. Subarray beam traces for a selection of explosions and earthquakes. The identification at the extreme left refers to Tables 1 and 2. The vertical lines indicate the splitting of each beam trace into the N, S, C1, C2 and C3 time series as defined in Table 3.

error of the partial autocorrelations of order $p+1$ and higher is

$$\hat{\sigma}[\hat{A}(t)] \approx N^{-\frac{1}{2}} \qquad t > p.$$

Thus if $\hat{A}(t)$ is close to zero for all lags $t > p$, one may tentatively conclude that the process $X(t)$ is autoregressive of order p.

Using equations (4) and (5) $\hat{A}(t)$ was computed up to lag 18 for each of the 10 time series. The results are given in the leftmost parts of Figs 3 and 4, where the $2\hat{\sigma}$-error limits have been drawn in. It appears that as far as the properties of the partial autocorrelation function are concerned, a low order autoregressive model is suggested for all time series. The estimated order varies from 1 for the C1 explosion time series up to 5 for the C1 earthquake time series.

In Tables 4 and 5 are tabulated the estimates $\hat{a}_{k1}, \hat{a}_{k2}, \ldots, \hat{a}_{kk}$ of the autoregressive coefficients, these estimates being obtained from equations (4) and (5). The estimate $\hat{\sigma}_z^2$ of the variance σ_z^2 of the residual process is obtained from

$$\hat{\sigma}_z^2 = \frac{1}{N} \sum_{t=k}^{N} [\hat{Z}(t)]^2 \tag{6}$$

with

$$\hat{Z}(t) = X(t) - \hat{a}_{k1} X(t-1) - \ldots - \hat{a}_{kk} X(t-k). \tag{7}$$

The parametrization of $X(t)$ obtained in this way is of rather limited value if the residual process $\hat{Z}(t)$ of equation (7) is non-white. If $\hat{Z}(t)$ is non-white, we face a separate parametrization problem for $\hat{Z}(t)$, and we are back to where we started. On the other hand, if $\hat{Z}(t)$ is white, its second order properties are completely determined by the single parameter σ_z^2. Thus the fit of the autoregressive model is measured by the whiteness of $\hat{Z}(t)$. The autocorrelation function of $\hat{Z}(t)$ was estimated using the formula of equation (5) for $\hat{Z}(t)$. If the residual process is white, the standard error of the autocorrelation function of order one and higher is

$$\hat{\sigma}(\rho_z(t)) \approx N^{-\frac{1}{2}}.$$

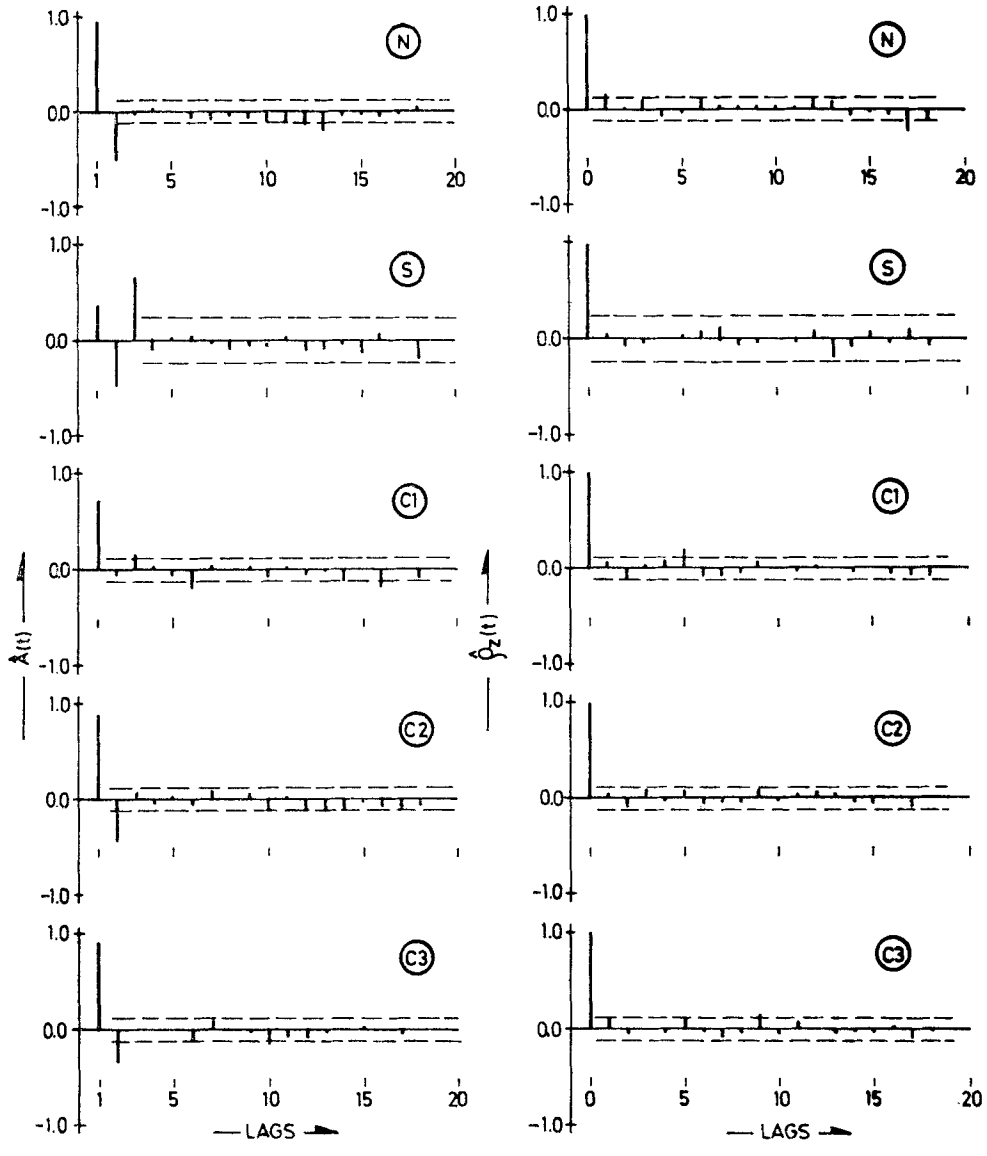

FIG. 3. Estimated partial autocorrelations $\hat{A}(t)$ and autocorrelations $\hat{\rho}_z(t)$ of the residual process $Z(t)$ for the N, S, C1, C2 and C3 subarray time series of explosion 22. The leftmost part of the figure shows estimated partial autocorrelations. The rightmost part of the figure shows estimated autocorrelations of the residual process using an autoregressive model of order k, where k is given in column 2 of Table 4.

The estimated autocorrelation function of the residual process is plotted with $2\hat{\sigma}$-limits in the rightmost parts of Figs 3 and 4. The fit of the estimated models appears to be quite satisfactory.

The estimating/fitting procedure was repeated for the remaining events listed in Tables 1 and 2. In the large majority of cases it was found that the events are described to a good approximation by low order autoregressive models, the order varying in most cases between 2 and 6, with the lower order coefficients being significantly

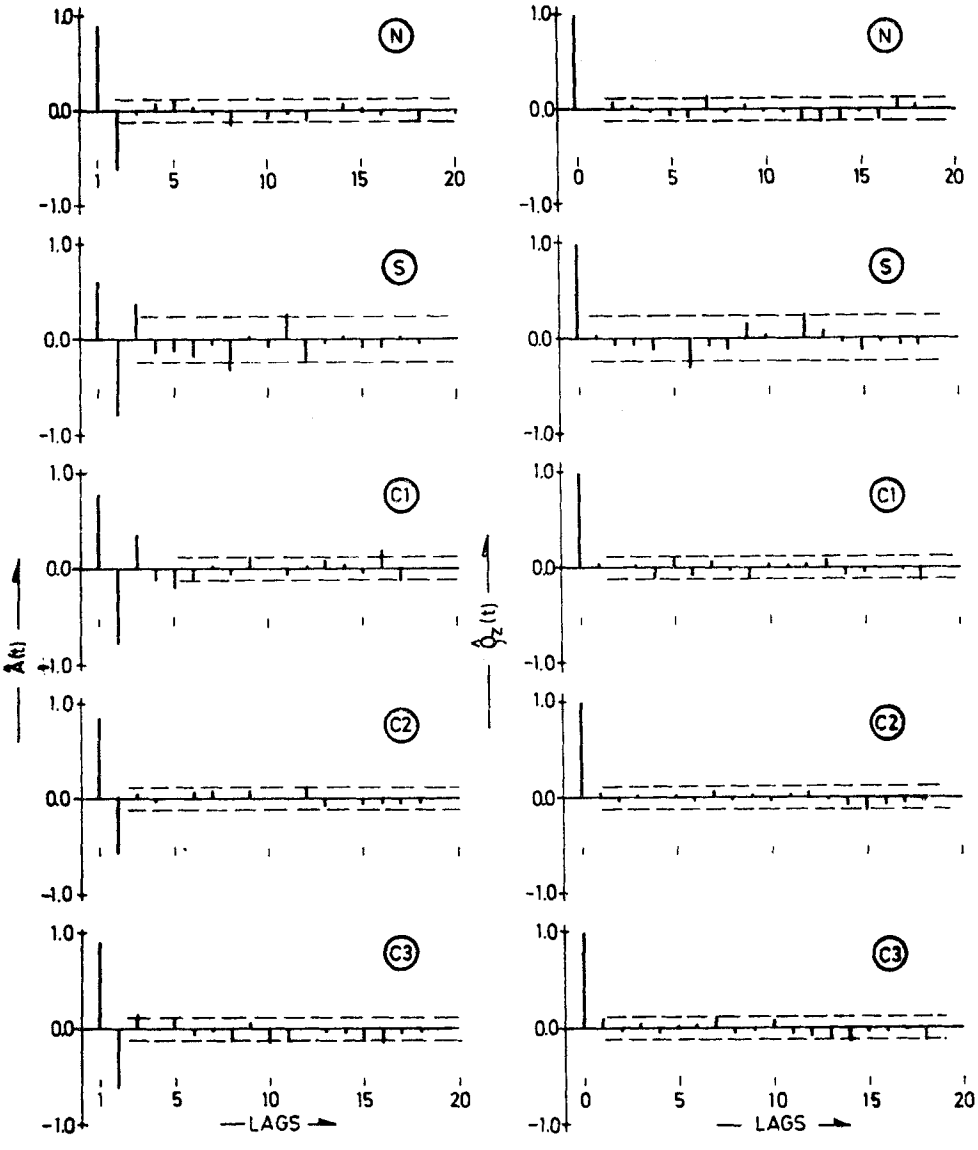

FIG. 4. Same as in Fig. 3 but with data from earthquake 10.

smaller in absolute value than the two higher order coefficients. Also, when successively fitting higher order models, the two higher order autoregressive coefficients were found to be approximately constant from iteration 3 on.

Let $\hat{\mathbf{a}} = \hat{a}_{k1}, \hat{a}_{k2}, \ldots, \hat{a}_{kk}$ be the vector of estimated coefficients for a particular time series. Then an estimate (see Box & Jenkins 1970) of the covariance matrix is given by

$$\hat{V}(\hat{\mathbf{a}}) = N^{-1}\left(1 - \sum_{t=1}^{k} \hat{\rho}(t)\hat{a}_{kt}\right)\hat{P}^{-1}$$

where $\hat{P}$ is the $k \times k$ matrix given on the left-hand side of equation (4). Typically we found that $\hat{\sigma}(\hat{a})$ takes its values in the range from 0·04 to 0·10 for the N, C1, C2 and C3 series and from 0·08 to 0·17 for the S series.

Table 4

Estimated autoregressive parameters for the N, S, C1, C2 and C3 time series of explosion 22. The order of the autoregressive model for each of the time series involved is determined from the corresponding partial autocorrelations as given in Fig. 3

	Order	$\hat{a}_{k1}$	$\hat{a}_{k2}$	$\hat{a}_{k3}$	$\hat{\sigma}_z^2$
N	2	1·47	−0·52	—	8308
S	3	0·84	−0·83	0·66	199692
C1	1	0·73	—	—	86000
C2	2	1·08	−0·22	—	33467
C3	2	1·24	−0·34	—	22083

Table 5

Same as in Table 4, but with data from earthquake 10

	Order	$\hat{a}_{k1}$	$\hat{a}_{k2}$	$\hat{a}_{k3}$	$\hat{a}_{k4}$	$\hat{a}_{k5}$	$\hat{\sigma}_z^2$
N	2	1·41	−0·64	—	—	—	8464
S	3	1·34	−1·19	0·38	—	—	80846
C1	5	1·64	−1·31	0·29	0·21	−0·20	27387
C2	2	1·33	−0·63	—	—	—	13007
C3	2	1·42	−0·64	—	—	—	13310

5. Reduction to a 3rd order model and the problem of short-period discriminants

In the remaining part of this work we will look more closely at eventual differences in second-order structure for nuclear explosions and earthquakes. For matters of comparison and computation it is convenient to have a standard model for all events. An attempt was therefore made to fit a 3rd order autoregressive model to all events. The autoregressive coefficients $\hat{a}_{31}, \hat{a}_{32}, \hat{a}_{33}$ were estimated using equations (4) and (5) with $k = 3$. The results are given for the N, S and C1 series (using data from the same subarray as in Section 4) in Tables 6 and 7.

In most cases the residual process was found to be approximately white when a 3rd order model was used. As explained in Section 2 the variance parameter σ_z^2 describes a scaling factor in the spectrum only and is not very useful for discrimination purposes. It is interesting to plot the power spectrum (see Figs 5 and 6) as computed from the formula (3) with $p = 3$ for the N, S and C1 series of the explosion and earthquake considered in the preceding section. Also, in Figs 5 and 6 we have plotted the power spectrum as computed in the 'ordinary' way using a Fast Fourier Transform algorithm. The two curves representing the two different power spectral estimates are seen to agree fairly well in the frequency range from 0·2 Hz up to the cut-off frequency $f_c = 5$ Hz, showing that a 3rd order model is capable of reproducing quite well the essential power spectral features in this frequency range. For frequencies lower than 0·2 Hz, when using a 3rd order model, the formula of equation (3) seems to result in larger values for the power spectrum than the estimate of the power spectrum computed from the Fast Fourier Transform. It is difficult to evaluate the significance of this difference, since the power spectrum estimates are not too reliable for such low frequencies, and the effect of a finite sample size starts to make itself felt here. This is especially true for the S series containing only 65 samples.

Before discussing the problem of discrimination, it is interesting to look at the time evolution of a typical explosion and a typical earthquake as described by the autoregressive coefficients. This roughly corresponds to a time-frequency diagram showing the evolution in time of the power spectrum of the event. Time-frequency diagrams have been used by a number of scientists, but they are difficult to interpret and use for discrimination purposes because of their complexity. The time evolution plot of

Table 6

Estimated autoregressive coefficients for the N, S and C1 time series of the subarray beam traces for the explosions of Table 1. A 3rd order model has been assumed for each event. The mean value and standard deviation is obtained by averaging over the 40 events of Table 1

	Presumed explosions								
	Noise			Signal			Coda 1		
No.	$\hat{a}_{31}$	$\hat{a}_{32}$	$\hat{a}_{33}$	$\hat{a}_{31}$	$\hat{a}_{32}$	$\hat{a}_{33}$	$\hat{a}_{31}$	$\hat{a}_{32}$	$\hat{a}_{33}$
1	1·51	−0·86	0·10	0·99	−0·80	0·03	0·82	−0·72	0·18
2	1·39	−0·51	−0·05	0·93	−0·77	0·02	0·81	−0·55	0·10
3	1·24	−0·50	−0·05	0·63	−0·72	0·40	0·48	−0·68	0·19
4	1·59	−0·79	0·11	1·09	−0·85	0·24	0·82	−0·64	0·12
5	1·73	−1·16	0·30	−0·13	−0·40	−0·01	−0·09	−0·32	−0·26
6	1·26	−0·43	−0·04	0·72	−0·21	0·14	0·73	−0·27	−0·17
7	1·39	−0·63	0·04	1·12	−0·53	0·17	0·07	−0·40	0·08
8	1·72	−0·98	0·16	0·54	−0·95	0·41	0·86	−0·75	0·57
9	1·19	−0·19	−0·09	0·64	−0·97	0·51	0·77	−0·74	0·45
10	1·64	−0·81	0·07	0·80	−0·52	−0·03	0·60	−0·22	−0·21
11	1·84	−1·10	0·20	0·79	−0·47	−0·07	1·03	−0·70	0·28
12	1·86	−1·15	0·22	1·15	−1·04	0·74	1·32	−0·56	0·14
13	1·56	−0·56	−0·09	0·60	−0·18	−0·34	0·93	−0·66	0·01
14	1·40	−0·47	−0·12	0·52	−0·98	0·24	0·64	−0·75	0·17
15	1·69	−0·95	0·15	1·13	−1·05	0·32	0·85	−0·79	0·36
16	1·71	−1·02	0·11	0·69	−0·91	0·41	0·49	−0·58	0·10
17	2·01	−1·17	0·23	0·67	−0·93	0·02	0·96	−1·39	0·37
18	1·00	−0·11	−0·08	0·57	−0·78	0·18	0·28	−0·53	−0·05
19	1·15	−0·33	−0·05	0·84	−0·86	0·58	1·02	−0·70	0·43
20	1·62	−0·98	0·19	0·80	−0·93	−0·15	0·70	−0·43	0·05
21	1·36	−0·56	−0·05	0·50	−0·91	0·18	0·45	−0·70	0·20
22	1·46	−0·49	−0·02	0·84	−0·83	0·66	0·79	−0·19	0·17
23	1·22	−0·34	−0·01	1·49	−0·94	0·07	1·57	−1·07	0·18
24	1·56	−0·60	−0·07	0·85	−0·60	−0·06	0·89	−0·78	0·14
25	1·50	−0·63	−0·01	1·52	−0·81	0·12	0·47	−0·38	0·01
26	0·78	−0·24	−0·03	0·36	−0·10	0·18	0·46	−0·23	0·01
27	1·69	−0·86	0·12	0·57	−0·94	0·42	0·70	−0·63	0·43
28	1·54	−0·83	0·10	0·53	−0·31	−0·19	0·71	−0·44	−0·08
29	1·59	−0·95	0·20	1·18	−0·64	−0·07	1·22	−0·74	−0·04
30	1·38	−0·48	−0·08	1·54	−1·03	0·15	1·25	−0·67	−0·01
31	1·49	−0·71	0·02	0·95	−0·91	0·22	0·78	−0·60	0·20
32	1·30	−0·38	−0·15	0·97	−0·43	0·20	0·22	−0·02	0·15
33	1·80	−1·30	−0·34	0·78	−0·72	0·10	0·96	−0·81	0·25
34	1·37	−0·33	−0·18	1·22	−1·24	0·59	0·79	−0·43	−0·07
35	1·69	−0·79	0·05	0·77	−0·79	0·44	0·93	−0·39	0·30
36	1·57	−0·57	−0·06	0·46	−0·47	0·02	0·28	−0·15	0·17
37	1·62	−0·75	0·01	0·77	−0·82	0·14	0·69	−0·75	0·26
38	1·76	−0·98	0·16	0·67	−0·96	0·37	0·80	−0·37	0·25
39	1·18	−0·21	−0·18	0·59	−0·94	0·28	0·47	−0·77	0·16
40	1·47	−0·61	−0·00	0·94	−0·85	0·15	1·16	−0·95	0·24
Mean	1·50	−0·68	0·02	0·81	−0·75	0·19	0·74	−0·59	0·15
Sta. dev.	0·25	0·31	0·13	0·33	0·26	0·24	0·34	0·26	0·18

Fig. 7 concentrates the information of spectral shape changes into the autoregressive parameters. More detailed information of the changes of the autoregressive parameters can of course be obtained by further subdividing each event into a much larger number of (overlapping) sections. For our purposes the crude picture of Fig. 7 will be sufficient.

In Fig. 7 we have plotted the two high order autoregressive coefficients for the earthquake and explosion studied in Section 4. While the autoregressive coefficients

Table 7

Estimated autoregressive coefficients for the N, S and Cl time series of the subarray beam traces for the explosions of Table 2. A 3rd order model has been assumed for each event. The mean value and standard deviation is obtained by averaging over the 45 events of Table 2.

	Presumed earthquakes								
	Noise			Signal			Coda 1		
No.	$\hat{a}_{31}$	$\hat{a}_{32}$	$\hat{a}_{33}$	$\hat{a}_{31}$	$\hat{a}_{32}$	$\hat{a}_{33}$	$\hat{a}_{31}$	$\hat{a}_{32}$	$\hat{a}_{33}$
1	1·30	−0·36	−0·16	1·45	−0·87	0·02	1·70	−1·27	0·30
2	2·00	−1·43	0·37	1·57	−0·94	0·07	1·73	−1·38	0·42
3	1·41	−0·52	−0·05	1·91	−1·61	0·51	1·68	−1·37	0·37
4	1·52	−0·81	0·08	2·07	−1·77	0·54	1·87	−1·40	0·39
5	1·00	−0·25	−0·06	1·31	−0·93	0·13	1·37	−1·05	0·24
6	1·26	−0·51	−0·06	1·22	−0·62	−0·09	1·42	−0·77	0·01
7	1·32	−0·51	−0·08	1·55	−1·33	0·44	1·78	−1·39	0·37
8	1·30	−0·53	0·05	1·51	−1·19	0·30	1·79	−1·48	0·45
9	1·15	−0·31	−0·11	1·59	−1·02	0·11	1·11	−0·54	−0·06
10	1·38	−0·58	−0·04	1·34	−1·19	0·37	1·62	−1·26	0·37
11	1·33	−0·43	−0·05	1·46	−1·06	0·27	1·42	−0·86	0·05
12	1·16	−0·33	−0·20	1·29	−0·81	0·02	1·60	−1·16	0·25
13	1·16	−0·39	0·02	1·78	−1·28	0·26	1·48	−1·06	0·24
14	1·13	−0·26	−0·05	1·57	−1·11	0·24	1·47	−1·19	0·44
15	1·41	−0·68	0·05	1·69	−1·01	0·10	1·34	−0·92	0·30
16	1·32	−0·45	−0·03	1·52	−1·00	0·23	1·60	−1·03	0·22
17	0·87	0·21	−0·24	1·93	−1·46	0·38	1·80	−1·31	0·29
18	1·77	−1·01	0·15	0·70	−0·57	0·16	1·14	−0·65	0·08
19	1·35	−0·31	−0·14	1·40	−0·77	0·06	1·61	−1·08	0·26
20	1·85	−1·17	0·24	1·78	−1·29	0·29	1·93	−1·46	0·41
21	1·88	−1·17	0·23	1·43	−0·93	0·02	1·77	−1·39	0·39
22	1·46	−0·89	0·19	1·52	−1·09	0·25	1·48	−1·02	0·18
23	1·27	−0·41	−0·05	1·60	−1·20	0·38	1·74	−1·35	0·46
24	1·24	−0·63	0·10	1·50	−1·30	0·44	1·39	−1·09	0·27
25	0·67	0·40	−0·53	0·99	0·34	−0·55	1·04	−0·07	−0·34
26	1·35	−0·58	0·04	1·40	−0·67	−0·03	1·44	−0·71	0·01
27	1·38	−0·70	0·04	1·15	−0·74	0·16	1·25	−0·77	0·15
28	1·61	−0·88	0·14	0·95	−0·82	0·36	1·13	−0·93	0·19
29	1·50	−0·74	0·09	1·47	−1·00	0·29	1·45	−0·75	0·03
30	1·79	−1·20	0·29	0·67	−0·78	0·21	0·71	−0·71	0·03
31	1·68	−0·85	0·08	0·87	−0·40	0·04	1·12	−0·71	0·32
32	2·01	−1·53	0·43	1·61	−1·14	0·28	2·02	−1·67	0·53
33	1·88	−1·29	0·35	1·99	−1·63	0·47	1·72	−1·25	0·25
34	1·48	−0·76	0·07	2·09	−1·76	0·52	1·59	−1·04	0·12
35	1·84	−1·22	0·25	1·91	−1·64	0·59	1·90	−1·56	0·55
36	1·49	−0·44	−0·12	1·39	−0·78	0·17	1·62	−0·97	0·25
37	1·90	−1·02	0·09	1·43	−0·64	0·11	1·91	−1·16	0·21
38	1·18	−0·12	−0·16	1·26	−0·41	−0·13	1·02	−0·16	−0·09
39	1·59	−0·83	0·08	1·57	−1·41	0·47	1·71	−1·41	0·50
40	1·66	−1·08	0·26	1·64	−1·39	0·45	1·65	−1·23	0·37
41	1·10	−0·31	−0·06	2·05	−1·77	0·59	1·74	−1·25	0·28
42	1·54	−0·85	0·11	1·46	−0·93	0·14	1·61	−1·08	0·27
43	1·34	−0·38	−0·13	1·76	−1·44	0·45	1·90	−1·48	0·41
44	1·45	−0·57	−0·09	1·60	−1·02	0·18	1·55	−0·93	0·17
45	1·51	−0·66	−0·04	1·97	−1·68	0·48	1·75	−1·46	0·41
Mean	1·44	−0·65	0·03	1·51	−1·07	0·24	1·55	−1·08	0·25
Sta. Dev.	0·30	0·40	0·18	0·34	0·42	0·22	0·28	0·35	0·18

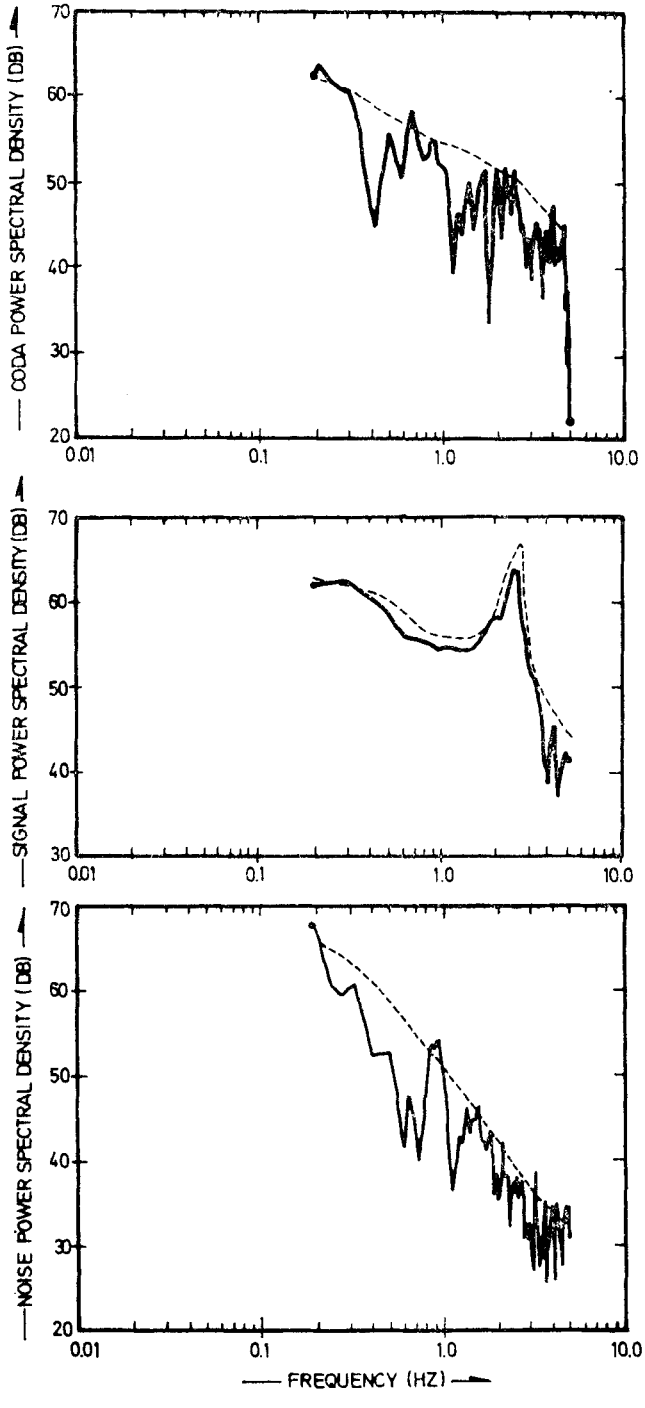

FIG. 5. Estimated power spectral densities of the N, S and C1 subarray time series of explosion 22. The solid lines represent power spectral estimates using a Fast Fourier Transform algorithm with subsequent smoothing. The dashed lines represent power spectral estimates based on equation (3). The dashed curves have been shifted 3 DB units upwards relative to the solid curves to get the estimates well separated.

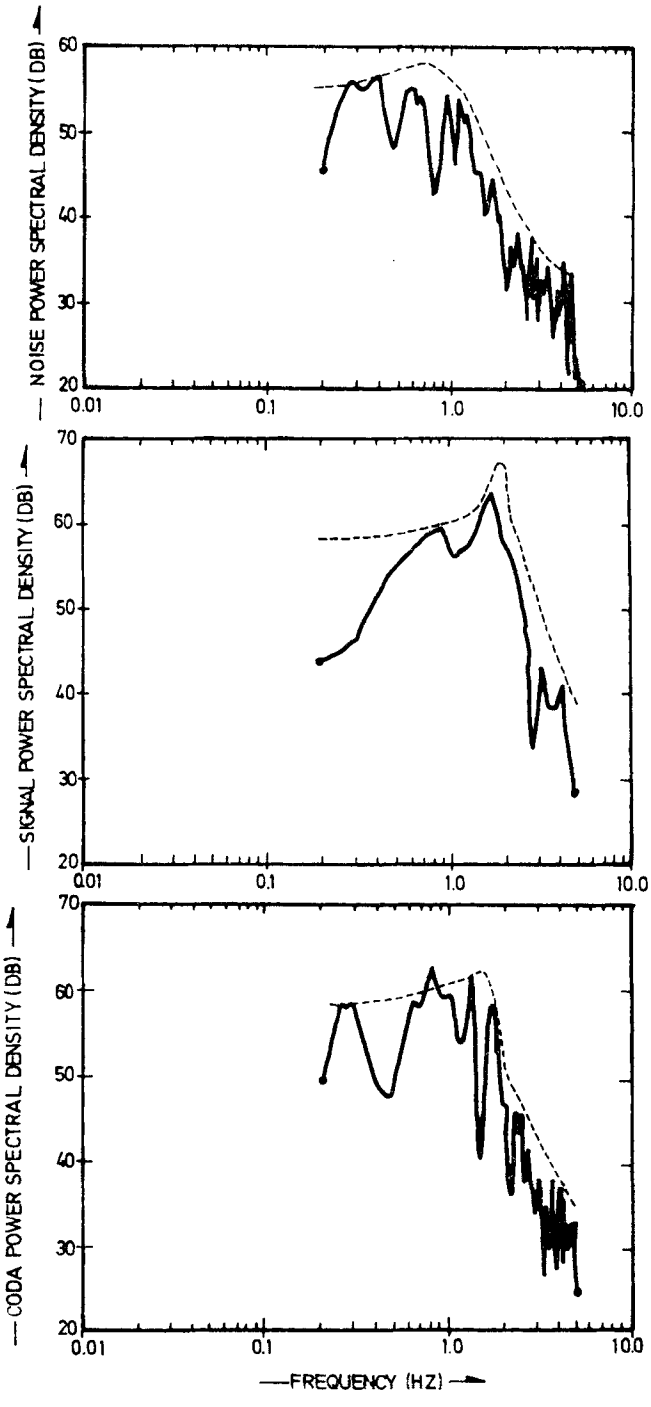

FIG. 6. Same as in Fig. 5, but with data from earthquake 10.

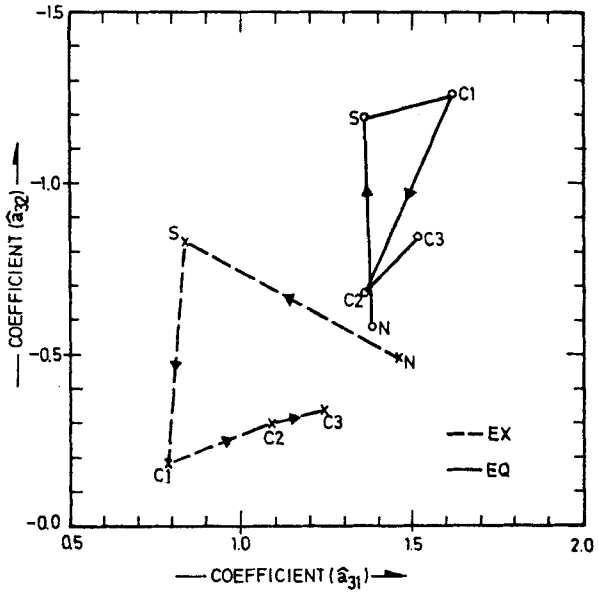

FIG. 7. Time evolution in terms of estimated autoregressive coefficients $\hat{a}_{31}$ and $\hat{a}_{32}$ for explosion 22 and earthquake 10. A 3rd order model

$$X(t)-a_{31}\,X(t-1)-a_{32}\,X(t-2)-a_{33}\,X(t-3) = Z(t)$$

has been assumed. The symbols N, S, C1, C2 and C3 are used to denote the values of $\hat{a}_{31}$ and $\hat{a}_{32}$ for the N, S, C1, C2 and C3 subarray time series.

for the noise preceding the two events are almost identical, the coefficients for the earthquake sharply increase in absolute value when the signal arrives, the opposite being the case for the explosion. Maximum separation is seen to occur for the C1 portion of the events. Moving further back into the coda (the C2 and C3 coefficients) it is clear that most of the separation effect has disappeared, and we are rapidly approaching the state where the coefficients take the value they had for the noise time series. On the basis of this plot we infer that the C2 and C3 time series are of limited importance for discrimination purposes, and that the C1 series and its autoregressive coefficients appear to be best suited for obtaining a good discriminant.

Unfortunately, but not unexpectedly, the rather dramatic separation of the two events of Fig. 7 is not universal. This is immediately revealed by a quick inspection of Tables 6 and 7. However, what is clear from these tables and the mean values computed there, is that the plots of Fig. 7 represent some sort of average time evolution behaviour for the explosion and earthquake data set considered. From the computed mean values and standard deviations one may conclude that the C1 time series and its autoregressive coefficients are slightly better suited for discrimination than the S time series. Another strong argument supporting this conclusion is that the S series has a relatively small sample size (65 samples as compared to 235 samples for the C1 series), this resulting in a larger uncertainty in the estimation procedure as is clear from the plots of the error limits in Figs 3 and 4.

From a study of the C1 coefficients of Tables 6 and 7 it is clear that the lower order coefficient $\hat{a}_{33}$ is of limited value for discrimination purposes. An eventual discriminant would therefore to a large extent have to be based on the two higher order coefficients $\hat{a}_{31}$ and $\hat{a}_{32}$. A plot of these coefficients is given in Fig. 8. It appears from the plot that a complete separation of explosions and earthquakes contained in our data set cannot be obtained using these coefficients.

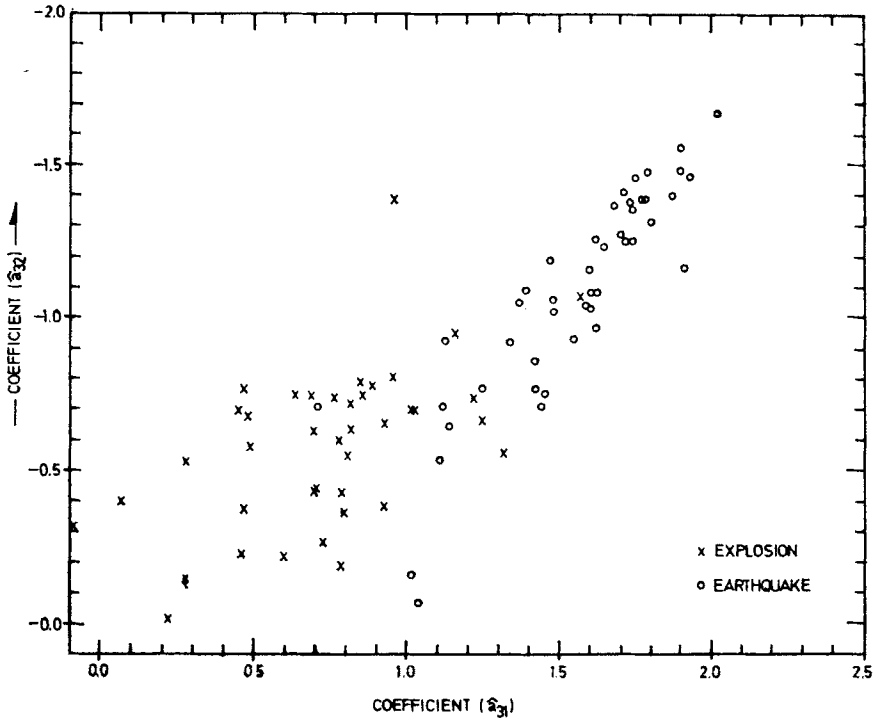

FIG. 8. Estimated 3rd order autoregressive coefficients $\hat{a}_{31}$ and $\hat{a}_{32}$ for the C1 subarray beam time series for the events of Tables 1 and 2.

Unfortunately, the atypical events of Fig. 8 cannot simply be ignored because the fit to a 3rd order model is poor. Consider for example earthquake 18 (from Northern Sinkiang), earthquake 31 (Iran) and explosion 30 (Tadzhik). For all of these events the fit to a 3rd order model varies from good to excellent. However, in terms of autoregressive coefficients the earthquakes tend to behave like explosions and vice versa. It should be noted also that with the possible exception of earthquake 31 these events have a low value for the coefficient $\hat{a}_{33}$ not used in Fig. 8. A plot of the subarray beam traces for these events is given in Fig. 2.

Also for the Eastern Kazakh area atypical events do occur, see for example explosion 12. Though this event has values for $\hat{a}_{31}$ and $\hat{a}_{32}$ that tend to be centred away from the explosion population, the time evolution of the coefficients resembles that of an explosion, the S and C1 coefficients having lower absolute value than the coefficients for the noise preceding the event. This fact might suggest that the high absolute value of $\hat{a}_{31}$ and $\hat{a}_{32}$ is due to an extreme noise situation influencing the estimation procedure. One way of avoiding part of this effect would be to study instead the differences $b_{3i} = \hat{a}_{3i}(\mathrm{C1}) - \hat{a}_{3i}(N)$; $i = 1, 2$. The parameters b_{31} and b_{32} have been plotted in Fig. 9. It is clear, however, that the overall situation is not markedly improved from that of Fig. 8.

It is widely accepted that the $m_b(M_s)$ method comparing the relative excitation of body and surface waves is the most effective discriminant of shallow earthquakes and underground nuclear explosions. However, this method has its limitations, the most serious one possibly being the difficulty of measuring M_s for events of low magnitude. These difficulties have led a number of researchers (e.g. Weichert 1971; Anglin 1972; Israelson 1972) to consider discriminants based solely on short-period data. It seems fair to state that the short-period discriminants considered this far have been inferior

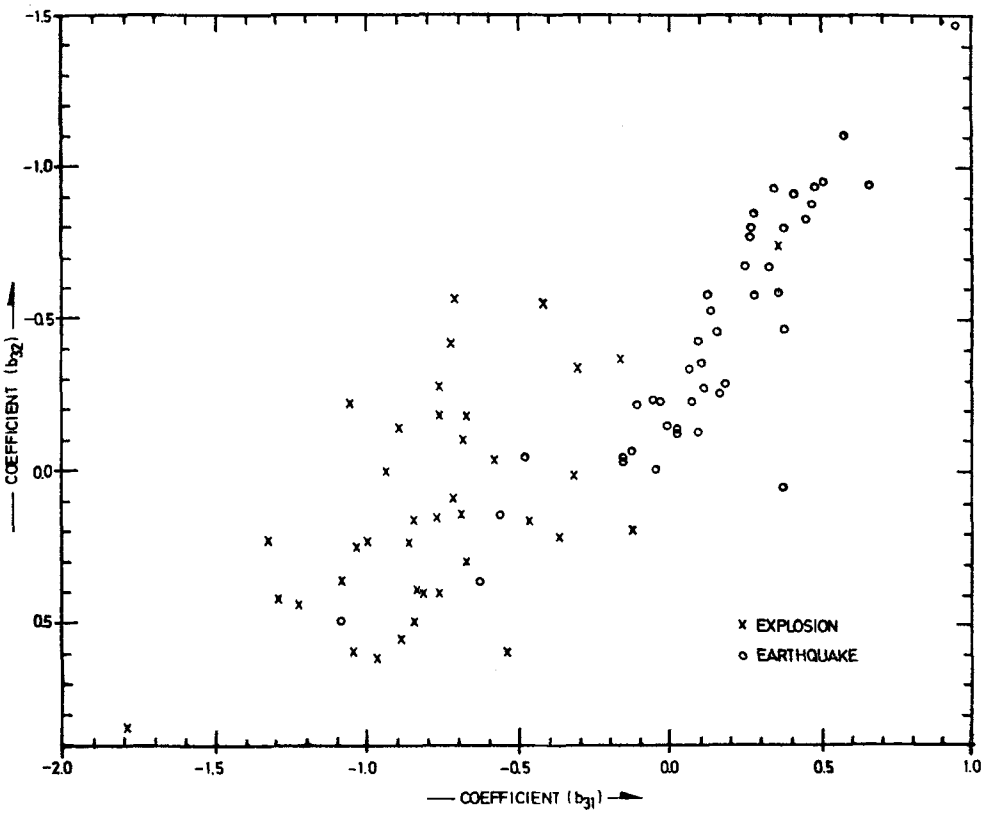

FIG. 9. Estimated parameters $b_{3i} = \hat{a}_{3i}(\mathrm{C1}) - \hat{a}_{3i}(\mathrm{N})$, $i = 1, 2$, for the events of Tables 1 and 2. A 3rd order model has been assumed for each event, and the data are from subarray 10C.

to the $m_b(M_s)$ discriminant in overall performance. However, it has not been entirely clear how much of the information inherent in the short-period structure of the data has actually been utilized using discriminants such as complexity and third moment of frequency (see Israelson 1972, for definitions). Thus, given these two discrimination parameters for a particular event, it is not clear to what degree it would be possible to reconstruct for example the power spectrum of the event.

On the basis of the evidence in this section it is tempting to conclude (see also Section 6, however) that an effective discriminant cannot be obtained using all available second-order information, that is, using properties of the autocorrelation function or equivalently the power spectrum of the short-period data. It is the autoregressive analysis which permits us to form this conclusion. This analysis concentrates the second-order information in a few parameters, and in principle therefore the study of discriminants using second-order properties should reduce to a study of these parameters, that is, essentially to a study of the plots in Figs 8 and 9. Though these plots do not necessarily represent the optimal use of the autoregressive parameters, it appears that no reasonable transformation or combination of $\hat{a}_{31}$ and $\hat{a}_{32}$ will result in anything resembling a complete separation for the considered data set.

6. Discussion

In this section some of the assumptions and approximations used in the preceding

analysis will be re-examined. Some of the possibilities that exist for improving our methods will also be briefly discussed.

(a) *Random signal model*

In developing the autoregressive scheme a random signal (time series) model was assumed for each event. This assumption is not absolutely essential since the autoregressive coefficients as computed using equation (4) depend on the autocorrelation function only, and this concept is well defined for a deterministic signal as well. However, it may be worthwhile stressing that our model is entirely based on second-order properties. All phase information is lost. Two events having the same amplitude spectrum (same autocorrelation function) but different phase spectra will have the same set of autoregressive parameters. So strictly speaking our study does not cover eventual discriminants based on phase spectrum information. Similarly for a random signal model all probabilistic information not pertaining to second moment structure is lost.

(b) *Analysis on the array beam*

For some of the weaker events (earthquakes nos 22 and 26 are good examples) the coefficients for the N, S and C1 series are virtually identical. This is due to the fact that the signal is almost completely masked by noise. The study of Section 5 was carried out on subarray beam level. This means that we have not utilized the full noise suppressing power of the array. The reason for working on the subarray beam rather than on the array beam was that array beam forming leads to a suppression of the coda, as well as a loss of higher frequency energy, it being anticipated this might result in loss of information. To check this argument, the analysis of Sections 4 and 5 was repeated on the array beam. Again the fit to a 3rd order model was found to be fairly good for most of the events. A selection of 3rd order autoregressive coefficients are given in Tables 8 and 9. Even though the coefficients for a particular event may vary considerably from those of Tables 6 and 7, the general explosion/earthquake trends are approximately the same. As indicated by the plot (see Fig. 10) of the two most significant coefficients of the C1 series, the situation with respect to discrimination is roughly the same as for the subarray beam analysis. Differences $b_{3i} = \hat{a}_{3i}(\mathrm{C1}) - \hat{a}_{3i}(N)$; $i = 1, 2$, were formed also for the array beam, but did not lead to significant improvements.

Table 8

Estimated 3rd order autoregressive coefficients for the N, S and C1 time series of the array beam trace for a selection of events from Table 1. The mean value and standard deviations are obtained by averaging over the 40 events of Table 1.

	Presumed explosions								
	Noise			Signal			Coda 1		
No.	$\hat{a}_{31}$	$\hat{a}_{32}$	$\hat{a}_{33}$	$\hat{a}_{31}$	$\hat{a}_{32}$	$\hat{a}_{33}$	$\hat{a}_{31}$	$\hat{a}_{32}$	$\hat{a}_{33}$
1	1·24	−0·47	−0·02	1·21	−1·16	0·33	1·09	−0·95	0·28
10	1·52	−0·44	−0·13	0·94	−0·62	−0·02	0·89	−0·58	0·00
12	1·43	−0·34	−0·15	1·19	−1·22	0·68	1·48	−0·82	0·29
13	1·63	−0·68	−0·02	1·16	−0·69	−0·00	0·99	−0·66	0·08
22	1·55	−0·57	−0·03	0·80	−0·74	0·04	1·06	−0·57	0·23
30	1·54	−0·70	0·08	1·30	−0·71	0·01	1·58	−1·13	0·20
Mean	1·37	−0·48	−0·02	1·00	−0·74	0·13	0·96	−0·73	0·14
Sta. dev.	0·28	0·29	0·12	0·29	0·34	0·22	0·32	0·26	0·15

Table 9

Estimated 3rd order autoregressive coefficients for the N, S and C1 time series of the array beam trace for a selection of events from Table 2. The mean value and standard deviations are obtained by averaging over the 45 events of Table 2.

	Presumed earthquakes								
	Noise			Signal			Coda 1		
No.	$\hat{a}_{31}$	$\hat{a}_{32}$	$\hat{a}_{33}$	$\hat{a}_{31}$	$\hat{a}_{32}$	$\hat{a}_{33}$	$\hat{a}_{31}$	$\hat{a}_{32}$	$\hat{a}_{33}$
10	1·23	−0·30	−0·11	1·57	−1·36	0·47	1·32	−0·91	0·12
18	1·43	−0·43	−0·12	1·19	−1·16	0·48	1·55	−1·26	0·34
22	2·04	−1·66	0·48	0·93	−0·32	−0·11	1·87	−1·43	0·36
26	1·28	−0·50	0·11	1·16	−0·42	−0·13	1·40	−0·64	0·05
31	1·44	−0·55	−0·03	0·80	−0·02	−0·04	1·46	−0·89	0·06
33	1·66	−0·86	0·09	1·78	−1·51	0·51	1·81	−1·52	0·47
Mean	1·32	−0·49	0·01	1·44	−1·00	0·24	1·64	−1·24	0·32
Sta. dev.	0·32	0·41	0·17	0·31	0·42	0·24	0·25	0·32	0·18

(c) *Other means of noise reduction*

It is not clear how much of the noise is actually removed by computing b_{3i}. The time series obtained by taking the differences of the C1 and N series, if autoregressive at all, in general will have autoregressive coefficients completely different from the coefficients b_{3i}. In general the noise and the signal may be assumed to be uncorrelated so that the autocorrelation functions are related by

$$\rho_{N+S}(t) = \rho_N(t) + \rho_S(t).$$

What has been used in equations (4) and (5) is $\hat{\rho}_{N+S}(t)$. One may think that a possible method of adjusting for the noise is to use instead $\hat{\rho}_S(t) = \hat{\rho}_{N+S}(t) - \hat{\rho}_N(t)$ and similarly for the C1, C2 and C3 series. In practice it turns out that this does not work (possibly the difficulties may be due to non-stationarities of the noise). For some of the events the function $\hat{\rho}_{N+S}(t) - \hat{\rho}_N(t)$ does not even define a legitimate autocorrelation function (it does not have its maximum at zero lag). The computations based on equation (4) then immediately break down.

We have used non-filtered data in our investigation, the motivation again being that we do not want to lose any information. Applying an appropriate band pass filter leads to improvements of the signal-to-noise ratio. However, the results of our test runs indicated that the filtered process is much more difficult to fit to an autoregressive scheme, both in terms of order of the model and whiteness of the residual process.

As a general comment to noise suppression techniques, we remark that although they may ultimately lead to some improvements with respect to discrimination, we consider it extremely unlikely that they will remove all difficulties. This is because several of the atypical events of Figs 8, 9 and 10 have a very high signal-to-noise ratio, indicating that the identification problems associated with these events are due to their particular second-order structure rather than being due to a low signal-to-noise ratio.

(d) *Possible improvements using a larger data base and combined criteria*

We have used the short-period data from NORSAR only. It is not unlikely that improvements of discrimination capability can be obtained by fitting autoregressive models to data from other stations and combining them into a multivariate discriminant. Combining short-period discrimination data from different stations has been considered by Anglin & Israelson (1973). A more effective discriminant may also result if autoregressive parameters were combined with $M_s(m_b)$ data. Using short-

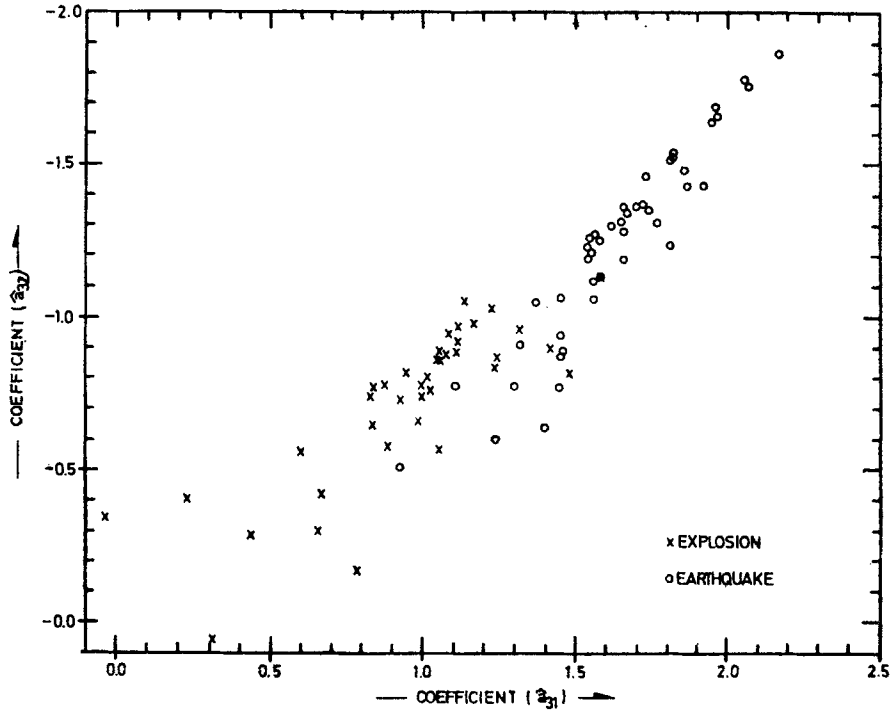

FIG. 10. Estimated 3rd order autoregressive coefficients $\hat{a}_{31}$ and $\hat{a}_{32}$ for the C1 array beam time series for the events of Tables 1 and 2.

period discriminant data as a supplement to the $M_s(m_b)$ discriminant has been suggested before among others by Basham & Anglin (1973) and Dahlman *et al.* (1974).

Acknowledgments

I am grateful to Dr E. S. Husebye and Dr H. Bungum for a number of very valuable suggestions on an earlier version of the manuscript. These suggestions have contributed significantly to the final form of the paper. Also I wish to thank Dr Bungum for the opportunity to use a data set prepared by him.

This research was supported by the Advanced Research Projects Agency of the Department of Defense and was monitored by AFTAC/VSC, Patrick AFB FL 32925, under contract no. F-08606-74-C-0049.

NTNF/NORSAR,
Post Box 51,
N-2007 *Kjeller,*
Norway.

References

Anglin, F. M., 1972. Short period discrimination studies using the Yellowknife seismological array data, *Proceedings Seismology and Seismic Arrays*, NORSAR, Kjeller, Norway.

Anglin, F. M. & Israelson, H., 1973. Discrimination of earthquakes and explosions using multistation seismic data, *Bull. seism. Soc. Am.*, **63**, 321–323.

Basham, P. W. & Anglin, F. M., 1973. Multiple discriminant screening procedure for test ban verification, *Nature* **246**, 474–476.

Box, G. E. P. & Jenkins, G. M., 1970. *Time series analysis forecasting and control*, Holden–Day, San Francisco.

Bungum, H., Husebye, E. S. & Ringdal, F., 1971. The NORSAR array and preliminary results of data analysis, *Geophys. J. R. astr. Soc.*, **25**, 115–126.

Dahlman, O., Israelson, H., Austegard, A. & Hörnström, G., 1974. Definition and identification of seismic events in the USSR in 1971, *Bull. seism. Soc. Am.*, **64**, 607–636.

Israelson, H., 1972. Seismic identification using short-period Hagfors data, *Proceedings Seismology and Seismic Arrays*, NORSAR, Kjeller, Norway.

Lacoss, R. T., 1971. Data adaptive spectral analysis methods, *Geophysics*, **36**, 661–675.

Peacock, K. L. & Treitel, S., 1969. Prediction deconvolution: Theory and practice, *Geophysics*, **34**, 155–169.

Tjøstheim, D., 1975. Some autoregressive models for short-period seismic noise, *Bull. seism. Soc. Am.*, **65**, 677–692.

Weichert, D. H., 1971. Short period spectral discriminant for earthquake and explosion differentiation, *Z. Geophysik*, **37**, 147–152.